Derivation and Application of a Conserved Orbital Energy for the Inverted Pendulum Bipedal Walking Model

Jerry E. Pratt and Sergey V. Drakunov

***Abstract*— We present an analysis of a point mass, point foot, planar inverted pendulum model for bipedal walking. Using this model, we derive expressions for a conserved quantity, the "Orbital Energy", given a smooth Center of Mass trajectory. Given a closed form Center of Mass Trajectory, the equation for the Orbital Energy is a closed form expression except for an integral term, which we show to be the first moment of area under the Center of Mass path. Hence, given a Center of Mass trajectory, it is straightforward and computationally simple to compute phase portraits for the system. In fact, for many classes of trajectories, such as those in which height is a polynomial function of Center of Mass horizontal displacement, the Orbital Energy can be solved in closed form.**

Given expressions for the Orbital Energy, we can compute where the foot should be placed or how the Center of Mass trajectory should be modified in order to achieve a desired velocity on the next step.

We demonstrate our results using a planar biped simulation with light legs and point mass body. We parameterize the Center of Mass trajectory with a fifth order polynomial function. We demonstrate how the parameters of this polynomial and step length can be changed in order to achieve a desired next step velocity.

I. Introduction

Bipedal walking is difficult to analyze mathematically because the equations of motion are nonlinear, high dimensional, and a hybrid mixture of continuous and discrete dynamics. In addition, the foot-ground contact forces have friction-limited, unilateral constraints. Due to these difficulties, simplified models of bipedal walking have been explored. Many of these models have proven very useful for both analysis and control.

One such simplified model is the Linear Inverted Pendulum Model of Kajita and Tanie [8]. In this model, a biped is approximated as a point mass with point feet and a Center of Mass trajectory that is constrained to a line for planar walking, or to a plane for three dimensional walking, i.e., the derivative of height with respect to forward motion or sideways motion is constant. With these constraints, the equations of motion become linear and a conserved orbital energy, the "Linear Inverted Pendulum Energy" can be derived. For example, for constant height sagittal plane walking,

$$\ddot{x} = \frac{g}{z_c} x$$

Jerry Pratt is with Florida Institute for Human and Machine Cognition, Pensacola, Florida 32502, USA *(jpratt@ihmc.us)*

Sergey V. Drakunov is with Florida Institute for Human and Machine Cognition, Pensacola, Florida 32502, and Tulane University, New Orleans, Louisiana 70118 USA *(drakunov@ieee.org)*

$$E_{LIP} = \frac{1}{2}\dot{x}^2 - \frac{g}{2z_c}x^2 \tag{1}$$

where x is the horizontal displacement from the foot to the Center of Mass, z_c is the constant Center of Mass height, g is the gravitational acceleration constant, and E_{LIP} is the Linear Inverted Pendulum energy. Similar results have been derived for three dimensional walking [6].

Given expressions for the Linear Inverted Pendulum Energy, state space phase portraits can then be determined as they consist of curves, each corresponding to constant values of the orbital energy. If one assumes a lossless transfer of support on each step, one can then determine where to place the foot in order to achieve a new Linear Inverted Pendulum Energy, and hence the velocity on the next step. Therefore, the Linear Inverted Pendulum model gives closed form expressions of where to step in order to achieve a next step velocity. While it is only a simplified model of walking, it has been applied, as an approximation, to several bipeds that do not hold all of the assumptions used in deriving the model [7], [8].

While the Linear Inverted Pendulum model is a useful model for determining foot placement, one of its main drawbacks is that the Center of Mass trajectory is linear. In this paper, we relax the Center of Mass trajectory constraint and only constrain the trajectory to be continuous. We derive a new expression for a conserved quantity during single support, which we refer to in this paper simply as the "Orbital Energy",

$$E_{orbit} = \frac{1}{2}\dot{x}^2 h^2(x) + g x^2 f(x) - 3g\int_0^x f(\xi)\xi d\xi \tag{2}$$

where

$$h(x) = f(x) - f'(x)x \tag{3}$$

where $z = f(x)$ is the Center of Mass height as a function of the horizontal displacement from the foot to the Center of Mass, $f'(x)$ is the derivative of $f(x)$ with respect to x and g is the acceleration of gravity.

Like the Linear Inverted Pendulum Energy equation, this expression for Orbital Energy allows us to determine where to step to achieve a next step velocity, but without assuming a linear height trajectory. While it still requires the assumption of a point mass body and a point foot, we believe that its application to more complicated bipeds will be successful for several reasons including the following,

- Bipedal walking is an inherently robust problem, not requiring precision, accuracy, or repeatability. Hence

errors resulting from the use of simplified models can often be tolerated.
- Any errors introduced from the use of a simplified model often converge to an acceptable steady state error. Though a simple model may not result in a perfect controller, the choice of a good model will result in one whose feedback is qualitatively correct and quantitatively sufficient.
- There are many redundant opportunities for control in bipedal walking beyond the choice of footsteps. For example, modulating the Center of Pressure on the feet, distributing forces between legs during the double support phase, and accelerating internal inertia can all be used to control velocity during walking.

In the next Sections we detail the derivation of Equation 2, show example trajectories and phase portraits, including closed form expressions for polynomial trajectories, and present simulations verifying our results.

II. Inverted Pendulum Dynamic Model

The xz-plane dynamics of the inverted pendulum model rotating around the origin $x = 0$, $z = 0$ is

$$M\ddot{x} = F\frac{x}{\sqrt{x^2+z^2}} \quad (4)$$

$$M\ddot{z} = -Mg + F\frac{z}{\sqrt{x^2+z^2}}, \quad (5)$$

where F is the translational knee force.

Let us assume that the force F maintains the constraint $z = f(x)$ between the variables x and z, where $f(x)$ is a function describing the Center of Mass trajectory in the xz-plane. We treat this constraint as a manifold in the system's 4-dimensional space defined by $\sigma = z - f(x) = 0$.

Differentiating σ twice we have:

$$\begin{aligned}\ddot{\sigma} &= \ddot{z} - f'(x)\ddot{x} - f''(x)\dot{x}^2 \\ &= F\frac{1}{M\sqrt{x^2+z^2}}[z - f'(x)x] - g - f''(x)\dot{x}^2 \quad (6)\end{aligned}$$

If $\sigma(t) \equiv 0$ then $\dot{\sigma} \equiv 0$ and $\ddot{\sigma} \equiv 0$, and, hence,

$$F\frac{1}{\sqrt{x^2+z^2}} = M\frac{g + f''(x)\dot{x}^2}{z - f'(x)x},$$

or

$$F = M\sqrt{x^2+z^2}\frac{g + f''(x)\dot{x}^2}{z - f'(x)x}. \quad (7)$$

In order to keep the state on the manifold $\Sigma = \{\sigma = z - f(x) = 0\} \cap \{\dot{\sigma} = \dot{z} - f'(x)\dot{x} = 0\}$ the amplitude of the force F which creates the constraint should be not greater than the maximum permissible force F_{max}: $\|F\| \le F_{max}$. We also require that the foot should not leave the ground, so F should be nonnegative:

$$0 \le M\sqrt{x^2+z^2}\frac{g + f''(x)\dot{x}^2}{z - f'(x)x}x \le F_{max}.$$

Substituting Equation 7 into Equation 4, and since on the manifold Σ we have $z \equiv f(x)$, the equation of constrained motion along the x-axis is:

$$\ddot{x} = \frac{g + f''(x)\dot{x}^2}{f(x) - f'(x)x}x \quad (8)$$

We now consider a few particular simple cases to verify Equation 8. In the following Sections we study in more detail the cases when $f(x)$ is a polynomial of x.

Case I: If $f(x) = z = const$ then, as one can see from Equation 8, we obtain the Linear Inverted Pendulum Dynamics presented in Equation I,

$$\ddot{x} = \frac{g}{z}x.$$

Case II: If the horizontal velocity is a constant, $\dot{x} = v = const$, then

$$\dot{v} = 0 \Rightarrow g + f''(x)v^2 = 0 \Rightarrow f''(x) = -\frac{g}{v^2}.$$

and hence $f(x)$ will be a parabola. Assuming that the starting x-point is x_0 and the final point is x_1 and, correspondingly, z_0 and z_1 are starting and final heights, we have

$$f(x) = -\frac{g}{2v^2}(x - x_0)(x - x_1) + z_0\frac{x - x_1}{x_0 - x_1} + z_1\frac{x - x_0}{x_1 - x_0}.$$

If $-x_0 = x_1$ and $z_0 = z_1$:

$$f(x) = -\frac{g}{2v^2}(x^2 - x_0^2) + z_0.$$

As can be easily seen such motion is a free fall with constant x-speed (assuming there are no losses). The force F, in this case, is zero since in Equation 7 the term $g + f''(x)\dot{x}^2 = 0$.

Case III: If $f(x) = \sqrt{r^2 - x^2}$, or $x^2 + z^2 = r^2$ is a semicircle, where $r = const$, then in this case the easiest way to derive the motion equation is to use the polar coordinates

$$x = r\sin(\theta) \quad (9)$$

$$z = r\cos(\theta), \quad (10)$$

where θ is the angle between the direction to the point (x, z) and the vertical direction. It satisfies the equation

$$J\ddot{\theta} = rMg\sin(\theta),$$

where $J = Mr^2$, hence

$$\ddot{\theta} = \frac{g}{r}\sin(\theta).$$

This is the equation of the standard inverted pendulum with constant length, and together with Equation 9 it is equivalent to Equation 8 in this case.

III. The Solution of the Dynamic Equations of Motion

In this section we derive an exact first integral of the general constrained Equation (8), resulting in Equation 2 presented in the Introduction.

Let us write Equation 8 in the standard state-space form:

$$\dot{x}_1 = x_2 \quad (11)$$

$$\dot{x}_2 = \frac{g + f''(x_1)x_2^2}{f(x_1) - f'(x_1)x_1}x_1, \quad (12)$$

where $x_1 = x$, and $x_2 = \dot{x}$.

Considering x_1 as the independent variable, the system (11)-(12) can be written as one equation:

$$\frac{dx_2}{dx_1} = \frac{g + f''(x_1)x_2^2}{[f(x_1) - f'(x_1)x_1]x_2}x_1, \tag{13}$$

or returning to the original notation for $x_1 = x$, and using a new notation $Y(x) = x_2^2 = \dot{x}^2$ we obtain

$$\begin{aligned} Y'(x) &= 2\frac{g + f''(x)Y(x)}{[f(x) - f'(x)x]}x \\ &= \frac{2xf''(x)}{f(x) - f'(x)x}Y(x) + \frac{2gx}{f(x) - f'(x)x}. \end{aligned} \tag{14}$$

Equation 14 is a linear first order differential equation with a variable coefficient with respect to the unknown function $Y(x)$:

$$Y'(x) = \phi(x)Y(x) + \psi(x), \tag{15}$$

where

$$\phi(x) = \frac{2xf''(x)}{f(x) - f'(x)x},$$

and

$$\psi(x) = \frac{2gx}{f(x) - f'(x)x}.$$

The solution of (15) can be written as

$$Y(x) = \Phi(x, x_0)Y(x_0) + \int_{x_0}^{x} \Phi(x, \xi)\psi(\xi)d\xi,$$

where $\Phi(x, x_0)$ is a fundamental solution:

$$\begin{aligned} \Phi(x, x_0) &= \exp\left[\int_{x_0}^{x} \phi(\xi)d\xi\right] \\ &= \exp\left[\int_{x_0}^{x} \frac{2\xi f''(\xi)}{f(\xi) - f'(\xi)\xi}d\xi\right] \\ &= \exp\left\{-2\int_{x_0}^{x} \frac{d[f(\xi) - f'(\xi)\xi]}{f(\xi) - f'(\xi)\xi}\right\} \\ &= \exp\left\{-2\log[f(x) - f'(x)x]\right. \\ &\quad \left. + 2\log[f(x_0) - f'(x_0)x_0]\right\} \\ &= \left[\frac{f(x_0) - f'(x_0)x_0}{f(x) - f'(x)x}\right]^2. \end{aligned} \tag{16}$$

Therefore, we have

$$\begin{aligned} Y(x) &= \left[\frac{f(x_0) - f'(x_0)x_0}{f(x) - f'(x)x}\right]^2 Y(x_0) \\ &+2g\int_{x_0}^{x} \left[\frac{f(\xi) - f'(\xi)\xi}{f(x) - f'(x)x}\right]^2 \frac{\xi}{f(\xi) - f'(\xi)\xi}d\xi \\ &= \left[\frac{f(x_0) - f'(x_0)x_0}{f(x) - f'(x)x}\right]^2 Y(x_0) \\ &+\frac{2g}{[f(x) - f'(x)x]^2}\int_{x_0}^{x} [f(\xi) - f'(\xi)\xi]\,\xi d\xi. \end{aligned} \tag{17}$$

The last equation means that

$$\begin{aligned} &\dot{x}^2[f(x) - f'(x)x]^2 - \dot{x_0}^2[f(x_0) - f'(x_0)x_0]^2 \\ &= 2g\int_{x_0}^{x} [f(\xi) - f'(\xi)\xi]\,\xi d\xi. \end{aligned} \tag{18}$$

Let's introduce a function $h(x)$ as

$$h(x) = f(x) - f'(x)x, \tag{19}$$

then (18) can be written as

$$\dot{x}^2h^2(x) - \dot{x_0}^2h^2(x_0) = 2g\int_{x_0}^{x} h(\xi)\xi d\xi. \tag{20}$$

Since

$$\begin{aligned} \int_{x_0}^{x} h(\xi)\xi d\xi &= \int_{x_0}^{x} [f(\xi) - f'(\xi)\xi]\,\xi d\xi \\ &= 3\int_{x_0}^{x} f(\xi)\xi d\xi - x^2f(x) + x_0^2f(x_0), \end{aligned} \tag{21}$$

we can write (18) as

$$\begin{aligned} &\frac{1}{2}\dot{x}^2h^2(x) - \frac{1}{2}\dot{x_0}^2h^2(x_0) \\ &= 3g\int_{x_0}^{x} f(\xi)\xi d\xi - gx^2f(x) + gx_0^2f(x_0), \end{aligned} \tag{22}$$

or

$$\begin{aligned} &\frac{1}{2}\dot{x}^2h^2(x) + gx^2f(x) - 3g\int_{x_0}^{x} f(\xi)\xi d\xi \\ &= \frac{1}{2}\dot{x_0}^2h^2(x_0) + gx_0^2f(x_0), \end{aligned} \tag{23}$$

Collecting all the terms dependent on x on the left hand side, and the terms dependent on the initial conditions on the right hand side we have

$$\begin{aligned} &\tfrac{1}{2}\dot{x}^2h^2(x) + gx^2f(x) - 3g\textstyle\int_0^x f(\xi)\xi d\xi \\ &= \tfrac{1}{2}\dot{x_0}^2h^2(x_0) + gx_0^2f(x_0) - 3g\textstyle\int_0^{x_0} f(\xi)\xi d\xi. \end{aligned} \tag{24}$$

We see that the left hand side of the last expression is a conserved quantity during the evolution of the dynamic equations of motion and is the Orbital Energy we introduced in the Introduction (2),

$$E_{orbit} = \frac{1}{2}\dot{x}^2h^2(x) + gx^2f(x) - 3g\int_0^x f(\xi)\xi d\xi$$

Thus, (24) can be interpreted as

$$\frac{dE_{orbit}}{dt} = 0.$$

IV. Velocity Control

Given the expression for Orbital Energy in Equation 2, we can determine where to step to achieve a desired next step velocity using the following method. If we let v_{des} be the desired velocity at the top of the next stride (when $x = 0$), then

$$E_{des} = \frac{1}{2}v_{des}^2h^2(0) \tag{25}$$

This is the Orbital Energy that needs to be achieved as a result of the step,

$$E_{des} = \frac{1}{2}\dot{x_0}^2h^2(x_0) + gx_0^2f(x_0) - 3g\int_0^{x_0} f(\xi)\xi d\xi \tag{26}$$

We then can solve Equations 25 and 26 for x_0, which gives us the location to step to achieve the desired velocity.

Note that if we assume lossless steps, then we can assume that the initial velocity of the next step ($\dot{x}_0$) equals the end of velocity of the current step. Otherwise, we need to use an impact model to determine the velocity loss due to impact.

The above method assumes that $f(x)$ and $h(x)$ are given. However, note that on each step we don't have to choose the same function $f(x)$ and we can adapt this function to the conditions on the next step. Although, to prevent the magnitude of the force F from becoming infinite, it is important to have smooth connections between steps so that on the next step the following conditions are fulfilled:

$$f_{old}(x_{1old}) = f_{new}(x_{0new}), \tag{27}$$

$$f'_{old}(x_{1old}) = f'_{new}(x_{0new}), \tag{28}$$

$$\dot{x}(t_{1old}) = \dot{x}(t_{0new}). \tag{29}$$

Here f_{old} and f_{new} are functions f on the previous and the next step, while x_{1old} and x_{0new} represent the same spatial point in the coordinate frame of the previous and the next step, respectively. Similarly, t_{1old} and t_{0new} is the same time moment when the new step is done.

The conditions (27) and (28) mean that there is no jump in the height of the center of gravity and the velocity vector direction, while (29) means that there is no jump in the velocity magnitude.

As a special case of velocity control, let us consider a problem of choosing the step size to stop the walking system. The system is stopped when the state trajectory reaches the origin of the constrained system phase space ($x = 0$, $\dot{x} = 0$). The phase trajectory which leads into the origin is defined by the points x_0 and $\dot{x}_0$, which correspond to an Orbital Energy of 0.0. This also corresponds to Equation 22 having a solution $x = 0$, $\dot{x} = 0$, i.e.

$$-\dot{x_0}^2 h^2(x_0) = 2g \int_{x_0}^{0} h(\xi)\xi d\xi \tag{30}$$

V. Polynomial Trajectories

Let us consider the situation with steady walking when the function f is the same on the next step $f_{new} = f_{old} = f$ and there is a "smooth connection" between steps so that conditions (27-29) are fulfilled.

Assume that the function $f(x)$ is a polynomial of order n :

$$f(x) = \sum_{i=0}^{n} a_i x^i.$$

The corresponding function $h(x)$ defined by (19) is

$$h(x) = f(x) - f'(x)x = \sum_{i=0}^{n} a_i(1-i)x^i. \tag{31}$$

and the integral portion of the Orbital Energy is

$$\int_0^x f(\xi)\xi d\xi = \sum_{i=0}^{n} \frac{1}{i+2} a_i x^{i+2} \tag{32}$$

Thus the Orbital Energy is a polynomial function of x. For different values of Orbital Energy, we get different functions

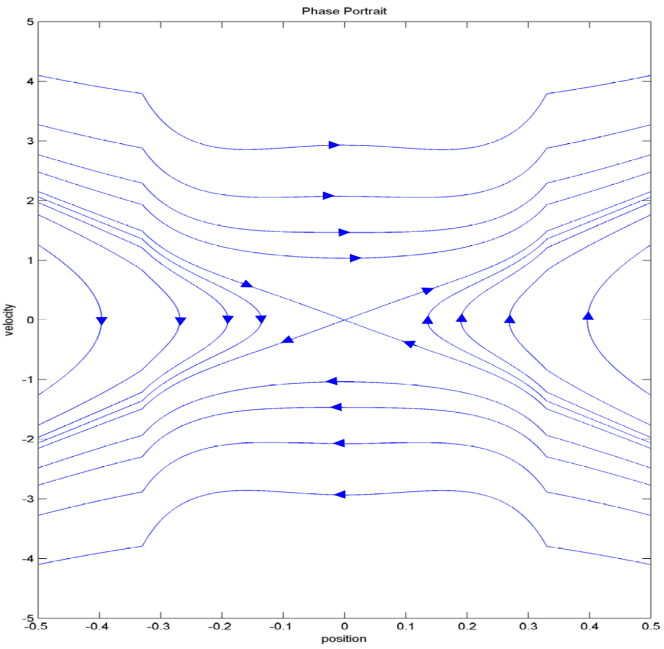

Fig. 1. Phase portrait for a symmetric 4th order polynomial function $f(x)$.

of horizontal velocity versus horizontal displacement. These level curves are the phase portrait of the dynamic equations of motion. In Figure 1 we show such a phase portrait for the polynomial trajectory $z = f(x) = a_0 + a_2x^2 + a_4x^4$ with $a_0 = 0.682$, $a_2 = -2.0$, $a_4 = 9.1827$. Outside the interval $-0.33 < x < 0.33$ then $f(x)$ is constant. The curves that enter and leave the origin correspond to Orbital Energy levels of 0.0. For a linear system, those curves would correspond to the stable and unstable eigenvectors of the system. For our system, which is nonlinear, those curves are not straight lines. In both cases however, the origin is a saddle point.

From $f(x_0) = f(x_1)$, and $f'(x_0) = f'(x_1)$ we have the following two equations for $n+1$ coefficients a_i:

$$\sum_{i=0}^{n} a_i(x_1^i - x_0^i) = 0 \tag{33}$$

$$\sum_{i=1}^{n} a_i i(x_1^{i-1} - x_0^{i-1}) = 0. \tag{34}$$

The third equation is obtained by substituting (31) into (22)

$$\sum_{i=0}^{n} a_i \frac{1-i}{i+2}(x_1^{i+2} - x_0^{i+2}) = 0, \tag{35}$$

As an example, if $n \leq 3$ then these equations are

$$\begin{aligned}
&a_1(x_1 - x_0) + a_2(x_1^2 - x_0^2) + a_3(x_1^3 - x_0^3) = 0 \\
&a_2 2(x_1 - x_0) + a_3 3(x_1^2 - x_0^2) = 0 \\
&a_0 \frac{1}{2}(x_1^2 - x_0^2) - a_2 \frac{1}{4}(x_1^4 - x_0^4) \\
&-a_3 \frac{2}{5}(x_1^5 - x_0^5) = 0
\end{aligned}$$

For symmetric legs, when $x_0 = -x_1$

$$\begin{aligned} a_1 x_1 + a_3 x_1^3 &= 0 \quad (36)\\ a_2 2 x_1 &= 0 \quad (37)\\ -a_3 \frac{2}{5} x_1^5 &= 0. \quad (38) \end{aligned}$$

This leaves only one possible solution $f(x) \equiv const = a_0$. So, we need to consider $n > 3$.

For $n \leq 5$ we have

$$\begin{aligned} &a_1(x_1 - x_0) + a_2(x_1^2 - x_0^2)\\ &+a_3(x_1^3 - x_0^3) + a_4(x_1^4 - x_0^4) + a_5(x_1^5 - x_0^5) = 0\\ &a_2 2(x_1 - x_0) + a_3 3(x_1^2 - x_0^2)\\ &+a_4 4(x_1^3 - x_0^3) + a_5 5(x_1^4 - x_0^4) = 0\\ &a_0 \frac{1}{2}(x_1^2 - x_0^2) - a_2 \frac{1}{4}(x_1^4 - x_0^4) - a_3 \frac{2}{5}(x_1^5 - x_0^5)\\ &-a_4 \frac{1}{2}(x_1^6 - x_0^6) - a_5 \frac{4}{7}(x_1^7 - x_0^7) = 0. \end{aligned}$$

For the symmetric legs, when $x_0 = -x_1$

$$\begin{aligned} a_1 2 x_1 + a_3 2 x_1^3 + a_5 2 x_1^5 &= 0 \quad (39)\\ a_2 4 x_1 + a_4 8 x_1^3 &= 0 \quad (40)\\ -\frac{4}{5} a_3 x_1^5 - \frac{8}{7} a_5 x_1^7 &= 0, \quad (41) \end{aligned}$$

or

$$\begin{aligned} a_1 + a_3 x_1^2 + a_5 x_1^4 &= 0 \quad (42)\\ a_2 2 + a_4 4 x_1^2 &= 0 \quad (43)\\ -\frac{1}{5} a_3 - \frac{2}{7} a_5 x_1^2 &= 0, \quad (44) \end{aligned}$$

Therefore, in this case, $f(x)$ has three free parameters. Choosing as these parameters the coefficients a_0, a_4 and a_5 this function can be written as

$$f(x) = a_0 + \frac{3}{7} x_1^4 a_5 x - 2 a_4 x_1^2 x^2 - \frac{10}{7} x_1^2 a_5 x^3 + a_4 x^4 + a_5 x^5.$$

As can be seen from this expression

$$f(x_1) = f(x_0) = f(-x_1) = a_0 - a_4 x_1^4.$$

The derivative of $f(x)$ is

$$f'(x) = \frac{3}{7} x_1^4 a_5 - 4 a_4 x_1^2 x - \frac{30}{7} x_1^2 a_5 x^2 + 4 a_4 x^3 + 5 a_5 x^4.$$

Correspondingly

$$f'(x_1) = f'(x_0) = f'(-x_1) = \frac{8}{7} x_1^4 a_5.$$

The corresponding function $h(x) = f(x) - f'(x)x$ is

$$h(x) = a_0 + 2 a_4 x_1^2 x^2 + \frac{20}{7} x_1^2 a_5 x^3 - 3 a_4 x^4 - 4 a_5 x^5. \quad (45)$$

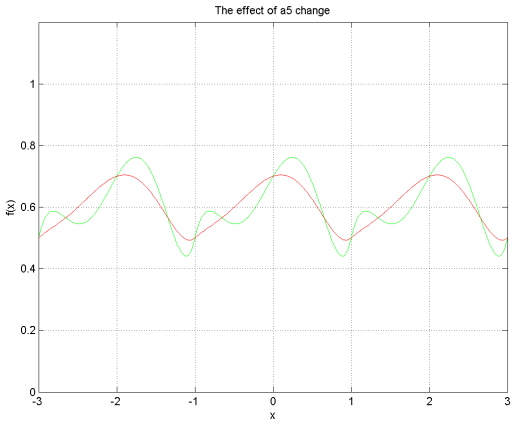

Fig. 2. Fifth order polynomial function $f(x)$, matching the "smooth connection" constraints, with differing values of a_5.

A. Stopping Condition for Polynomial Trajectories

We can derive the stopping condition for the polynomial trajectory using Equation 30,

$$-\dot{x}^2 h^2(x_0) = 2g \int_{x_0}^{0} h(\xi) \xi d\xi,$$

where x_0 in the new frame (with respect to the new rotation point) corresponds to the current x, when the new step is made.

We now assume a slightly more general situation when the command to stop comes not necessarily when the previous step is finished, but at an arbitrary moment at which the z-coordinate is z_0, and the horizontal and vertical velocities respectively are $\dot{x}_0$ and $\dot{z}_0$. Thus, if we assume further motion to satisfy the constraint $z = f_{new}(x)$ we have the following "smooth connection" conditions:

$$f_{new}(x_0) = z_0,$$

and

$$f'_{new}(x_0) = \frac{\dot{z}_0}{\dot{x}_0}.$$

Then for the polynomial

$$f(x) = \sum_{i=0}^{n} a_i x^i,$$

the corresponding constraints and the stopping condition (30) are

$$\begin{aligned} \sum_{i=0}^{n} a_i x_0^i &= z_0 \quad (46)\\ \sum_{i=1}^{n} i a_i x_0^{i-1} &= \frac{\dot{z}_0}{\dot{x}_0} \quad (47)\\ 2g \sum_{i=0}^{n} a_i \frac{1-i}{i+2} x_0^{i+2} &= \dot{x}_0 \left[z_0 - \frac{\dot{z}_0}{\dot{x}_0} x_0 \right]^2, \quad (48) \end{aligned}$$

In this case the minimum degree of a non-constant polynomial can be $n \leq 3$ and we have

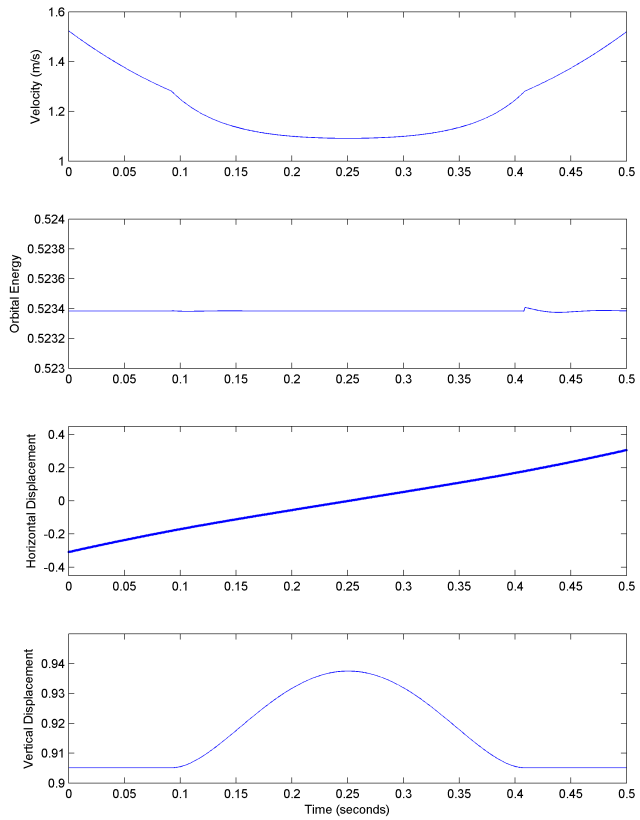

Fig. 3. Simulation results of single-leg, point mass, planar biped model showing horizontal velocity, Orbital Energy, horizontal displacement, and vertical displacement. Note that the Orbital Energy stayed constant to within 3 decimal places. Error beyond that is attributed to numerical effects of discrete simulation.

$$a_0 + a_1 x_0 + a_2 x_0^2 + a_3 x_0^3 = z_0 \quad (49)$$

$$a_1 + 2a_2 x_0 + 3a_3 x_0^2 = \frac{\dot{z}_0}{\dot{x}_0} \quad (50)$$

$$g a_0 x_0^2 - g\frac{1}{2} a_2 x_0^4 - g\frac{4}{5} a_3 x_0^5 = \dot{x}_0 \left[z_0 - \frac{\dot{z}_0}{\dot{x}_0} x_0 \right]^2 \quad (51)$$

These equations allow us to find the polynomial and the point x_0.

VI. Simulation Results

To validate our theoretical results, we performed a sequence of simulation experiments on two simulation models using the Yobotics Simulation Construction Set software package. The first model consisted of a free pin joint at the ground and an actuated translational leg joint, ending in a point mass body of $25.0kg$. The second model consisted of a planar biped with body mass of $25.0kg$, and legs with point mass feet, each of $0.05kg$. This model had rotational hip joints and translational knee joints.

In both systems, the support leg was actuated to control the body's height as a function of the horizontal distance from the foot to the body mass, using a proportional-derivative plus feed-forward computed torque command,

$$f_{knee} = k_z(f(x) - z) + b_z(f'(x)\dot{x} - \dot{z}) + M\sqrt{x^2 + z^2}\frac{g + f''(x)\dot{x}^2}{z - f'(x)x} \quad (52)$$

where k_z is the proportional gain and b_z is the derivative gain.

For the first model, the system was given appropriate initial conditions and controlled to follow $f(x)$. Because this model exactly matches the model which was used in the derivation of Equation 2, the Orbital Energy stayed constant to within 3 decimal points, as shown in Figure 3. This was verified for a variety of polynomial trajectories, thus validating Equation 2.

For the second model, we developed a control algorithm with the following characteristics:

- Track the Center of Mass height trajectory $f(x)$ using Equation 52, where $f(x)$ is constant when $|x| > x^*$. This will guarantee a smooth connection at exchange-of-support.
- Determine the next step distance by solving Equation 26 for x_0.
- Swing the swing leg to the desired step location using a proportional-derivative (PD) controller on the swing hip.
- Apply an equal and opposite hip torque to the support hip to prevent any pitch disturbance on the body.
- Place the swing leg when the horizontal displacement from the foot to the Center of Mass passes a desired exchange-of-support threshold. Ensure that the exchange-of-support threshold is large enough so that $f(x)$ is in a flat region ($|x| \geq x^*$). Also, delay exchange-of-support if necessary until the desired step location is in the flat region of $f(x)$.

To ensure a smooth connection, we used a symmetric polynomial $f(x) = a_0 + a_2 x^2 + a_4 x^4$ with $f(x) = z^*$ if $|x| \geq x^*$ where $x^* = \sqrt{\frac{-a_2}{2a_4}}$, corresponding to the point of zero slope of the polynomial.

Using this algorithm, we achieved walking with the planar biped model and were able to validate our theoretical results. Figure 4 shows results from a simulation in which the desired top-of-support velocity was changed between $0.0\frac{m}{s}$ to $1.5\frac{m}{s}$. The Center of Mass trajectory $f(x)$ stayed fixed with $a_0 = 0.9375$, $a_2 = -2.0$, and $a_4 = 30.864$, corresponding to $x^* = 0.18$ and $z^* = 0.9051$. The desired exchange-of-support horizontal displacement also stayed fixed at $0.25m$. We see that velocity tracking was quite accurate, the Orbital Energy was nearly constant during the support phase, exchange-of-support occurred at the desired value, except when it had to be delayed to accelerate the robot, and the Center of Mass height tracking was nearly perfect. Note that the desired Orbital Energy changed in proportion to the square of the desired velocity.

Figure 5 shows results from a simulation in which the desired exchange-of-support horizontal displacement was

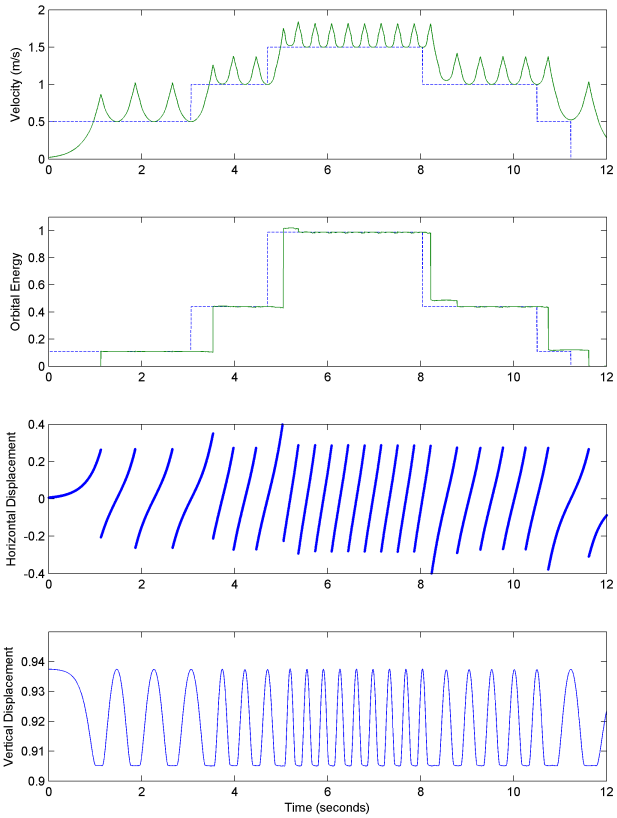

Fig. 4. Simulation results. The desired top-of-support horizontal velocity was changed between $0.0\frac{m}{s}$ and $1.5\frac{m}{s}$, while the desired polynomial Center of Mass trajectory and exchange of support horizontal displacement stayed fixed.

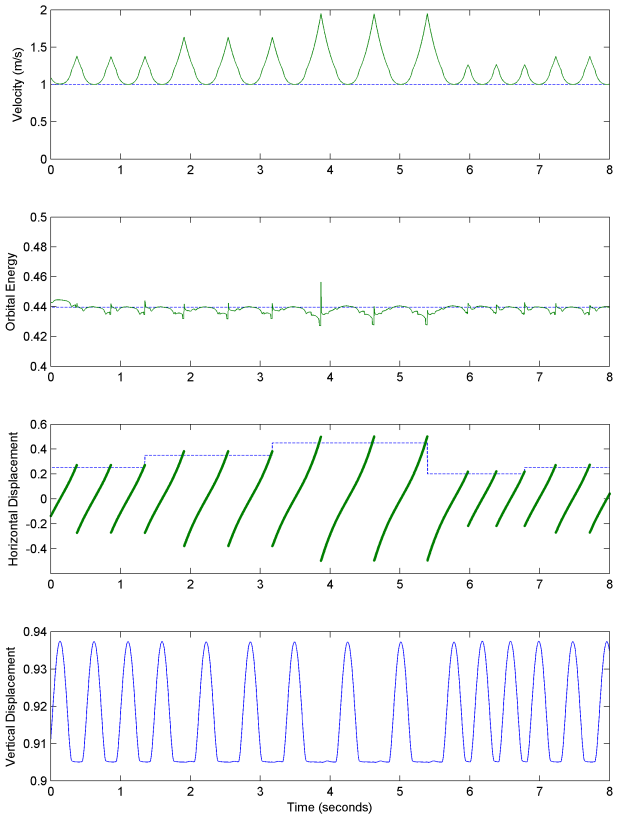

Fig. 5. Simulation results. The desired exchange of support horizontal displacement was changed between $0.25m$ and $0.45m$, while the desired top-of-support horizontal velocity and polynomial Center of Mass trajectory stayed fixed.

changed between $0.2m$ and $0.45m$, while the desired top-of-support velocity stayed fixed at $1.0\frac{m}{s}$ and the Center of Mass trajectory stayed fixed with the same values as in Figure 4. Again, we see that velocity tracking was quite accurate, the Orbital Energy was nearly constant during the support phase, and the Center of Mass height tracking was nearly perfect. Exchange-of-support occurred near the desired value, but there was some error due to control delays between determining it was time to place the foot and the time that foot placement actually occurred. Note that the desired Orbital Energy remained constant, as the desired top-of-support velocity and height remained constant.

Figure 6 shows results from a simulation in which the desired Center of Mass trajectory changed while the desired top-of-support velocity stayed fixed at $1.0\frac{m}{s}$ and the desired exchange-of-support displacement stayed fixed at $0.25m$. Again, we see that velocity tracking was quite accurate, the Orbital Energy was nearly constant during the support phase, exchange-of-support occurred near the desired value, and the Center of Mass height tracking was nearly perfect. Note that the desired Orbital Energy changed in proportion to the square of the desired top-of-support height.

VII. Conclusions and Future Work

We presented an analysis of the point mass, point foot, planar inverted pendulum model for bipedal walking, resulting in an expression for a conserved Orbital Energy. We then showed that the expression for Orbital Energy can be used to determine the next step location in order to control the next step velocity. This work was motivated by Kajita and Tanie's original Linear Inverted Pendulum Model [8] of walking, but extends on that model by not requiring a constant height or constant slope Center of Mass trajectory.

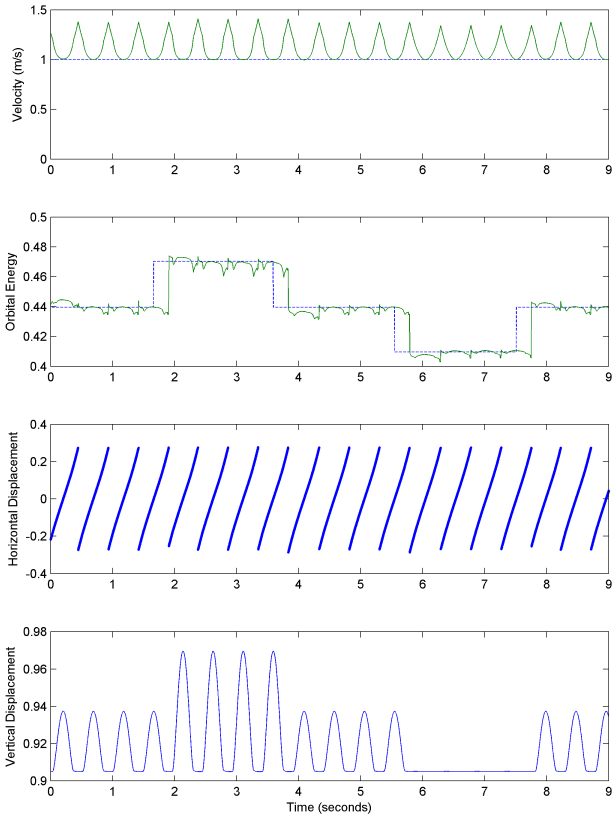

Fig. 6. Simulation results. The desired Center of Mass trajectory was changed while the desired top-of-support horizontal velocity and exchange of support horizontal displacement stayed fixed.

Following a function $z = f(x)$ fully constrains the internal configuration degrees of freedom of the robot, which has been shown by Grizzle, Chevallereau, Westervelt, and colleagues [1], [2], [3], [5] to allow the remaining lower degree-of-freedom dynamics to be more easily analyzed. Their prior work has shown that once the internal configuration degrees are constrained as a function of the unconstrained degrees of freedom, that a conserved Orbital Energy exists. In the general case, the conserved Orbital Energy is a very complicated expression. In this paper we showed that for the point-mass inverted pendulum model, the expression is fairly simple with only one simple integral that happens to be the first moment of area under the Center of Mass curve.

In another study [11], we extended the Linear Inverted Pendulum Model to include a flywheel body rather than a point mass body. With this "Linear Inverted Pendulum Plus Flywheel Model", we found closed-form expressions relating how angular momentum can be used to control velocity, and in particular how it can extend the "Capture Region", the region on the ground in which a biped can come to a stop if its foot is placed in that region.

Each extension of these simple models closes the gap between the model and the full dynamics of a bipedal robot. With each improvement we can more accurately compute things such as where to place the foot in order to achieve a next step velocity, or in order to regain balance after a disturbance. Next steps in this direction include:

- Extending the results of this paper to 3D walking.
- Combining the results from the Linear Inverted Pendulum plus Flywheel model to arbitrary Center of Mass trajectories.
- Applying the results of this paper to a real, rather than simulated, bipedal walking robot.

VIII. ACKNOWLEDGMENTS

Support for this work was provided by Honda Research Institute and the Office of Naval Research.

REFERENCES

[1] C. Chevallereau, G. Abba, Y. Aoustin, F. Plestan, E.R. Westervelt, C. Canudas-De-Wit, and J.W. Grizzle. Rabbit: a testbed for advanced control theory. *IEEE Control Systems Magazine*, 23(5):57–79, 2003.

[2] C. Chevallereau, A. Formal'sky, and D. Djoudi. Tracking a joint path for the walk of an underactuated biped. *Robotica*, 22(Part 1):15–28, 2004.

[3] M. Doi, Y. Hasegawa, and T. Fukuda. Passive dynamic autonomous control of bipedal walking. *Proceedings of the IEEE-RAS/RSJ International Conference on Humanoid Robots*, 2004.

[4] E.R. Dunn and R.D. Howe. Towards smooth bipedal walking. *Proceedings of the IEEE International Conference on Robotics and Automation*, pages 2489–2494, 1994.

[5] J.W. Grizzle, E.R. Westervelt, and C. Canudas-De-Wit. Event-based pi control of an underactuated biped walker. *42nd IEEE International Conference on Decision and Control*, pages 3091–3096, 2003.

[6] S. Kajita, F. Kanehiro, K. Kaneko, K. Yokoi, and H. Hirukawa. The 3d linear inverted pendulum mode: a simple modeling for a biped walking pattern generation. *Proceedings of the IEEE/RSJ International Conference on Intelligent Robots and Systems*, pages 239–246, 2001.

[7] S. Kajita and K. Tani. Experimental study of biped dynamic walking. *IEEE Control Systems Magazine*, 16(1):13–19, 1996.

[8] S. Kajita, K. Tani, and A. Kobayashi. Dynamic walk control of a biped robot along the potential energy conserving orbit. *Proceedings of the IEEE International Workshop on Intelligent Robots and Systems*, pages 789–794, 1990.

[9] J. Pratt. *Exploiting Inherent Robustness and Natural Dynamics in the Control of Bipedal Walking Robots*. PhD thesis, May 2000.

[10] J. Pratt, Chew Chee-Meng, A. Torres, P. Dilworth, and G. Pratt. Virtual model control: an intuitive approach for bipedal locomotion. *International Journal of Robotics Research*, 20(2):129–143, 2001.

[11] Jerry Pratt, John Carff, Sergey Drakunov, and Ambarish Goswami. Capture point: A step toward humanoid push recovery. *Proceedings of the IEEE-RAS/RSJ International Conference on Humanoid Robots*, 2006.